


Role of weak values in strong measurements

F. De Zela 

Departamento de Ciencias, Sección Física, Pontificia Universidad Católica del Perú, Apartado 1761, Lima 15088, Peru



(Received 8 September 2021; accepted 23 March 2022; published 4 April 2022)

The physical meaning of the quantum weak value still remains a matter of debate. Originally introduced by Aharonov *et al.* [*Phys. Rev. Lett.* **60**, 1351 (1988).] as another counterintuitive feature of quantum mechanics, it eventually evolved into a practical tool that is widely used. The theoretical framework in which weak values were introduced was given by von Neumann's model of quantum measurements. In this model, a system is submitted to measurement by coupling it to a "pointer," or meter. In the weak-coupling regime, one may perform a low-order Taylor expansion for the evolution operator of the system and meter. This standard approach ties weak values with weak couplings and weak measurements. We report closed-form expressions that can be used to untie weak values from weak measurements. The regime of strong measurements thereby becomes accessible to weak values, without leaving the framework in which the latter were originally introduced. The reported results should also help us to better understand the physical meaning of weak values.

DOI: [10.1103/PhysRevA.105.042202](https://doi.org/10.1103/PhysRevA.105.042202)

I. INTRODUCTORY REMARKS ON WEAK VALUES

Since their introduction in 1988 by Aharonov *et al.* [1], weak values have been and still remain a matter of debate. As up to now, one could say that "the quantum weak value has had an extensive and colorful theoretical history" [2]. This might have been caused by the way weak values were originally introduced, making reference to ontological views that were not actually captured by their mathematical definition. Indeed, the quantum weak value is defined as follows. Given an observable \hat{A} and two states, $|i\rangle$ and $|f\rangle$, the weak value of \hat{A} is the complex-valued quantity

$$A_w = \frac{\langle f|\hat{A}|i\rangle}{\langle f|i\rangle}. \quad (1)$$

As can be seen, despite the name and notation, there is nothing "weak" associated with the above definition, for which a more appropriate notation would be A_{fi} . State $|i\rangle$ is called the "preselected" state, and $|f\rangle$ is called the "postselected" state. To make sense of these names, one should consider the two states as being involved in a prepare-and-measure experiment [2], for which the probability of detecting $|f\rangle$ when $|i\rangle$ was prepared is given by $P = |\langle f|i\rangle|^2$. The name "weak" is, in turn, justified when, instead of \hat{A} , one considers the unitary operator $\hat{U}(\epsilon) = \exp(-i\epsilon\hat{A})$ acting on $|i\rangle$ and asks once again for the probability of detecting $|f\rangle$. This probability is now given by $P_\epsilon = |\langle f|\exp(-i\epsilon\hat{A})|i\rangle|^2$. The case when ϵ is very small then corresponds to a weak measurement [2]. In such a case, one may perform a Taylor series expansion to lowest order in ϵ , i.e., $\hat{U}(\epsilon) = \hat{I} - i\epsilon\hat{A} + \dots$, out of which various properties of weak-value measurements have been derived.

States $|i\rangle$ and $|f\rangle$ belong to some Hilbert space \mathcal{H}_S . Consider now that \mathcal{H}_S is a subspace of a larger space $\mathcal{H}_S \otimes \mathcal{H}_P$. This is the framework of Aharonov *et al.* [1]. Here, \mathcal{H}_S corresponds to the system being measured, and \mathcal{H}_P

corresponds to the measuring device, the "pointer" or meter. In this case, \hat{A} turns out to be part of the operator that rules the system-pointer interaction, i.e., a Hamiltonian \hat{H} that acts on $\mathcal{H}_S \otimes \mathcal{H}_P$. Following von Neumann's treatment of quantum measurements, one assumes that $\hat{H} = g\hat{A} \otimes \hat{P}$, where g is a coupling constant and \hat{P} has the meaning of an impulse operator, conjugate to the position degree of freedom that fixes the pointer's readout: $[\hat{X}, \hat{P}] = i$ (in units of $\hbar = 1$). In strong measurements, \hat{P} shifts the pointer's position to a place that is unambiguously correlated with an eigenvalue of \hat{A} . In this context, the unitary $\hat{U}(\epsilon)$ acquires the meaning of an evolution operator $\hat{U}(\epsilon) = \exp(-i\epsilon\hat{A} \otimes \hat{P})$, where $\epsilon = g\tau$ and τ is the pulselike interaction time. If we start with the system and meter being in an uncorrelated state $|\psi\rangle_S \otimes |x=0\rangle_P$, under the action of $\hat{U}(\epsilon)$ the system and meter get entangled [3]. Indeed, setting $|\psi\rangle_S = \sum_n c_n |a_n\rangle_S$, with $\hat{A}|a_n\rangle = a_n|a_n\rangle$, we get $\hat{U}(\epsilon)[|\psi\rangle_S \otimes |x=0\rangle_P] = \sum_n c_n |a_n\rangle_S \otimes |x=\epsilon a_n\rangle_P$. Measuring \hat{X} on subsystem P means reading out the pointer's position. The readout of the pointer's position disentangles the system-pointer state. Let us assume that the pointer's initial state $|x=0\rangle_P$ is centered in $x=0$ with a standard deviation σ . Whenever σ is much smaller than the spacings between a_n 's, the pointer's readout leaves subsystem S in a well-defined eigenstate of \hat{A} , whose corresponding eigenvalue unambiguously correlates with the pointer's position. This is the limit of strong measurements, i.e., when the pointer's wave function $\langle x|\phi\rangle_P$ consists of a series of nonoverlapping "spikes," whose centers coincide with the a_n 's [4]. The opposite limit refers to a weak measurement. In this case, the pointer's state is a superposition of strongly overlapping distributions, e.g., Gaussians, so that the pointer's readout is ambiguous, compatible with more than one eigenvalue a_n . A useless regime at first sight, the weak limit provides, in fact, a very powerful tool that has been variously exploited (see [2] and references therein). For example, it has been used as an

amplifier of very low signals [5]. It has also enabled the direct measurement of both the real and imaginary parts of quantum states [6], and it has helped to address counterintuitive features of quantum mechanics [7–9].

As already mentioned, various results related to weak values have been derived by going to lowest order in the Taylor expansion of $\hat{U}(\epsilon)$. For example, the real and imaginary parts of A_w can be related to shifts in the conjugate pointer variables [3]:

$$A_w = \frac{1}{\epsilon}(\langle \hat{X} \rangle + i4\sigma^2 \langle \hat{P} \rangle), \quad (2)$$

where the expectation values of \hat{X} and \hat{P} refer to the final pointer state. Because these conjugate variables do not commute, they cannot be measured simultaneously. Hence, $\text{Re } A_w$ and $\text{Im } A_w$ were first obtained from separate subensembles [6,10], and only recently were they simultaneously measured using two pointers, thereby avoiding noncommutativity [3,11].

Another example comes from considering the probabilities P_ϵ and P mentioned above. One can show [2] that

$$\frac{P_\epsilon}{P} = 1 + 2\epsilon \text{Im } A_w - \epsilon^2 (\text{Re } A_w^2 - |A_w|^2) + O(\epsilon^3). \quad (3)$$

The above expression, which is second order in ϵ , contains a second-order weak value A_w^2 . Generally, on using (1), n th-order weak values are defined as [2]

$$A_w^n = \frac{\langle f | \hat{A}^n | i \rangle}{\langle f | i \rangle}. \quad (4)$$

Already at second order in the Taylor expansion, some issues show up that should prompt us to seek an alternative approach. For example, if we choose $|f\rangle = |i\rangle$, then $A_w = \langle i | \hat{A} | i \rangle$, so that $\text{Im } A_w = 0$, and the lowest-order contribution of ϵ to Eq. (3) is second order. This contribution involves generally not only the real and imaginary parts of A_w but also the weak value of \hat{A}^2 as well. Hence, the simple choice $|f\rangle = |i\rangle$ has notorious consequences for P_ϵ/P , even though the definition of A_w does not prescribe any particular choice for states $|i\rangle$ and $|f\rangle$. The meaning of A_w —and of related quantities such as P_ϵ/P —should be independent of our choices of $|i\rangle$ and $|f\rangle$. The approach based on a Taylor expansion could then induce us to misinterpret the meaning of A_w in some cases. Besides this rather technical issue, we also notice a more physical one. Indeed, if we set \hat{A} equal to some Hamiltonian \hat{H} , taking again $|f\rangle = |i\rangle$ and setting $\epsilon = \Delta t$, Eq. (3) reads

$$P(\Delta t) = 1 - (\Delta t / \tau_Z)^2, \quad (5)$$

where $\tau_Z^{-2} \equiv (\Delta \hat{H})^2 = \langle i | \hat{H}^2 | i \rangle - \langle i | \hat{H} | i \rangle^2$. Put in this form, Eq. (3) acquires a physical meaning that has no essential links to weak values. Equation (5) lies, indeed, at the basis of the quantum Zeno effect [12]. Consider repeating the measurement of $|i\rangle$ N times. The probability $P^{(N)}(N\Delta t)$ that the system is found in $|i\rangle$ at time $N\Delta t$ approaches a value of 1 for large N . In that case, the system remains “frozen” in the initial state. This Zeno effect bears no meaningful connection to weak values.

There is, however, a very meaningful connection between quantum and classical weak-value measurements. The first experimental realization of a weak-value measurement was

made using classical light [13]. More than a decade later, the first quantum weak-value measurement was reported [14]. While in previous cases the system and meter were represented by two degrees of freedom of the same physical object, be it a photon or a classical light beam, in [14], two entangled photons were used. However, this proves only that weak values can *also* be measured on quantum objects, not that they are a unique quantum feature.

The above remarks suggest that the standard approach to weak values, which is based on a Taylor expansion, might have distorted somewhat their physical meaning, even though their usefulness as a versatile tool is beyond doubt. The purpose of this work is to help us better understand the essential meaning of weak values. To this end, we will present closed-form expressions that can be derived from von Neumann’s model of quantum measurements. Closed-form expressions are also useful for extending the domain of validity of weak values to include strong measurements. The latter were addressed previously [15–22], but mostly using a Taylor expansion in one form or another. It is worth mentioning that weak values have been interpreted in terms of forward- and backward-evolving states, a framework that allows us to address couplings of finite strength [21] as well as to distinguish between weak values and expectation values [23]. By applying this approach to the case in which the pointer state is given by a Gaussian distribution, one can derive expressions for the pointer’s shift which hold to all orders in the coupling strength [21]. While we also assume a Gaussian distribution for the pointer’s state, we rely on Eq. (1) as an operational definition of weak values, giving the symbols it contains their standard meaning.

The rest of this paper is organized as follows. In Sec. II, we present our main results, the detailed derivations of which are given in the Appendix. In Sec. III, we present some alternative forms of our main results. These forms should provide additional insight into the meaning of weak values. Section IV presents possible applications to Stokes polarimetry. The paper then closes with our conclusions.

II. CLOSED-FORM EXPRESSIONS INVOLVING WEAK VALUES

Let us focus on the emblematic case, originally addressed by Aharonov *et al.* [1], in which the system S is a two-state system. This can be physically realized by, e.g., spin-1/2 particles or, alternatively, by polarized light. The same mathematical formalism applies to all two-state systems, irrespective of their quantum or classical realization. Classical Jones vectors and spinors are mathematically the same, and the operators acting on them can be represented by two-dimensional matrices. We will use Dirac’s notation, without implying that our treatment is limited to the quantum case.

Let us consider a Hamiltonian \hat{H} and a system operator \hat{A} given by

$$\hat{H} = g\hat{P}\hat{A}, \quad \hat{A} = \mathbf{n} \cdot \boldsymbol{\sigma} \equiv \hat{\sigma}_n, \quad (6)$$

where \mathbf{n} is a unit vector and $\boldsymbol{\sigma}$ is the triple of Pauli matrices. For brevity, we drop, here and henceforth, the tensor-product symbol in operators and vectors that refer to $\mathcal{H}_P \otimes \mathcal{H}_S$. The

initial system-meter state $|i\rangle|\psi\rangle$ is given by

$$|i\rangle = \cos(\alpha/2)|+\rangle + e^{i\beta} \sin(\alpha/2)|-\rangle,$$

$$\langle x|\psi\rangle = \psi(x) = \frac{1}{(2\pi\sigma^2)^{1/4}} \exp\left(-\frac{x^2}{2\sigma^2}\right), \quad (7)$$

where $\sigma_z|\pm\rangle = \pm|\pm\rangle$. The state $|i\rangle$ is thus a general one whose representation on the Poincaré or Bloch unit sphere is the point $(\cos\beta \sin\alpha, \sin\beta \sin\alpha, \cos\alpha)$, while $\psi(x)$ represents a Gaussian distribution centered on $x = 0$, with σ being the rms width of $|\psi(x)|^2$.

We are interested in obtaining a closed-form expression for the unitary operator $\hat{U}(\epsilon) = \exp(-i\epsilon\hat{P}\hat{\sigma}_n)$. To this end, we use the following results, the derivations of which are given in the Appendix. First, it holds that

$$\exp(-i\theta\hat{\sigma}_n) = \frac{1}{2}\{(e^{-i\theta} + e^{i\theta})\hat{I} + (e^{-i\theta} - e^{i\theta})\hat{\sigma}_n\}, \quad (8)$$

where θ is any quantity that commutes with $\hat{\sigma}_n$. The second result reads

$$\sum_{k=0}^{\infty} \frac{(-\epsilon)^k}{k!} \frac{\partial^k \psi}{\partial x^k}$$

$$= \sqrt{2\sigma}(2\pi)^{1/4} \exp\left[-\frac{\epsilon^2}{4\sigma^2} + \frac{\epsilon x}{2\sigma^2}\right] G(x, \sigma\sqrt{2}), \quad (9)$$

where $G(x, \sigma) = |\langle x|\psi\rangle|^2$. On setting $\theta = \epsilon\hat{P}$ in (8) and considering that $\langle x|\hat{P}|\psi\rangle = -i\partial\psi/\partial x$, we can use (9) to get

$$\langle x|\exp(-i\epsilon\hat{P}\hat{\sigma}_n)|\psi\rangle$$

$$= \sqrt{2\sigma}(2\pi)^{1/4} \exp\left(-\frac{\epsilon^2}{4\sigma^2}\right)$$

$$\times G(x, \sigma\sqrt{2}) \left\{ \cosh\left(\frac{\epsilon x}{2\sigma^2}\right)\hat{I} + \sinh\left(\frac{\epsilon x}{2\sigma^2}\right)\hat{\sigma}_n \right\}. \quad (10)$$

The above equation yields

$$\frac{\langle f|\langle x|\exp(-i\epsilon\hat{P}\hat{\sigma}_n)|\psi\rangle|i\rangle}{\langle f|i\rangle}$$

$$= F(x, \epsilon, \sigma) \left\{ \cosh\left(\frac{\epsilon x}{2\sigma^2}\right) + \sinh\left(\frac{\epsilon x}{2\sigma^2}\right)\sigma_n^w \right\}, \quad (11)$$

where $F(x, \epsilon, \sigma) = \sqrt{2\sigma}(2\pi)^{1/4} \exp(-\epsilon^2/2\sigma^2)G(x, \sigma\sqrt{2})$ and σ_n^w is the weak value of $\hat{\sigma}_n$, as defined in (1). Equations (10) and (11) are two central results of this paper. They hold true, no matter how large ϵ might be, which means that σ_n^w can show up also in strong measurements. There is then hardly any reason to call σ_n^w a weak value. However, we will keep adhering to the standard nomenclature.

So far, we have worked in the x representation; that is, we have projected the pointer on the state $|x\rangle$. In connection with the protocol discussed in [1], this is often referred to as the step in which one performs a ‘‘strong’’ measurement. The system itself is instead subjected to a weak measurement. In the present context, such a distinction appears to be rather artificial. Anyhow, we can also project on an eigenstate $|p\rangle$ of the impulse operator. Following steps analogous to those used before, we get

$$\langle p|\exp(-i\epsilon\hat{P}\hat{\sigma}_n)|\psi\rangle = \tilde{\psi}(p)\{\cos(\epsilon p)\hat{I} - i\sin(\epsilon p)\hat{\sigma}_n\}, \quad (12)$$

where $\tilde{\psi}(p) = \langle p|\psi\rangle$ is the Fourier transform of $\psi(x)$, i.e., also a Gaussian. The above equation yields

$$\frac{\langle f|\langle p|\exp(-i\epsilon\hat{P}\hat{\sigma}_n)|\psi\rangle|i\rangle}{\langle f|i\rangle} = \tilde{\psi}(p)\{\cos(\epsilon p) - i\sin(\epsilon p)\sigma_n^w\}. \quad (13)$$

As we can see, the complex-valued quantity σ_n^w appears in both Eqs. (11) and (13). The left-hand sides of these equations have been the point of departure for various Taylor-series expansions. For instance, the probabilities P_ϵ and P referred to before can be calculated as follows.

In the x representation, we get

$$\frac{P_\epsilon}{P} = \frac{|\langle f|\langle x|\exp(-i\epsilon\hat{P}\hat{\sigma}_n)|\psi\rangle|i\rangle|^2}{|\langle f|i\rangle|^2|\psi(x)|^2}$$

$$= \exp\left[-\frac{\epsilon^2}{2\sigma^2}\right] \left\{ \cosh^2\left(\frac{\epsilon x}{2\sigma^2}\right) + \sinh\left(\frac{\epsilon x}{\sigma^2}\right) \operatorname{Re} \sigma_n^w \right.$$

$$\left. + \sinh^2\left(\frac{\epsilon x}{2\sigma^2}\right) |\sigma_n^w|^2 \right\}. \quad (14)$$

In the p representation, we get

$$\frac{P_\epsilon}{P} = \frac{|\langle f|\langle p|\exp(-i\epsilon\hat{P}\hat{\sigma}_n)|\psi\rangle|i\rangle|^2}{|\langle f|i\rangle|^2|\tilde{\psi}(p)|^2}$$

$$= \cos^2(\epsilon p) + \sin(2\epsilon p) \operatorname{Im} \sigma_n^w + \sin^2(\epsilon p) |\sigma_n^w|^2. \quad (15)$$

Taylor-series expansions of (14) and (15) yield, to lowest order in ϵ ,

$$\frac{P_\epsilon}{P} \approx 1 + \epsilon \frac{x}{\sigma^2} \operatorname{Re} \sigma_n^w, \quad (16)$$

$$\frac{P_\epsilon}{P} \approx 1 + 2\epsilon p \operatorname{Im} \sigma_n^w. \quad (17)$$

The above expressions were reported in [2] and constitute a basis, together with Eq. (2), for obtaining $\operatorname{Re} \sigma_n^w$ and $\operatorname{Im} \sigma_n^w$ from measurements performed in the x and p spaces, respectively. We see, therefore, that Taylor-series expansions can be misleading. They can lead us to conclude that the position variable has some inherent link with the real part of σ_n^w and, similarly, that the momentum variable has an inherent link with the imaginary part of σ_n^w . Equations (11) and (13) [or (14) and (15)] show that said links are not physically meaningful, just a coincidental consequence of the Taylor expansion. Furthermore, Eqs. (11) and (13) show that Taylor expansions in powers of ϵ do not involve different powers of σ_n^w . The commonly performed Taylor expansion of $\exp(-i\epsilon\hat{P}\hat{\sigma}_n)$ links ϵ^k with the k th-order weak value $\langle f|\hat{\sigma}_n^k|i\rangle/\langle f|i\rangle$. Regarding weak-value measurements, this may be seen as an artifact of the Taylor expansion. Moreover, the approach based on a series expansion can inspire generalizations that, while being fruitful [24], might contain limitations that derive from the approach itself rather than from the underlying physics. In contrast, analytic expressions can help a great deal in clarifying the true physical meaning of weak values [18,20,25].

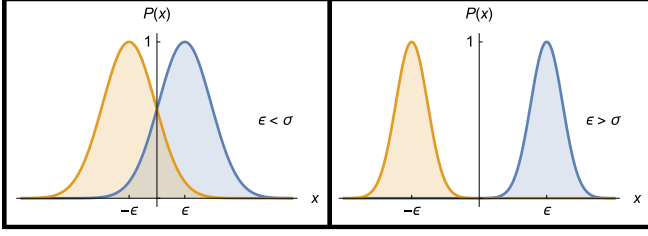


FIG. 1. Gaussian wave packets of a probe system that is used as pointer in von Neumann’s measurement model. Left: weak-coupling regime. The coupling strength between the probe and measured system is weak: $\epsilon \ll \sigma$. There is an overlap between probe distributions, so that they do not unambiguously correlate with the eigenvalues of the system’s observable. Right: strong-coupling regime, with $\epsilon \gg \sigma$. Each pointer’s readout is unambiguously correlated with one of the observable’s eigenvalues.

III. ALTERNATIVE FORMS OF OPERATORS AND PROBABILITIES

Equations (10) and (12) can be written in an alternative form:

$$\langle x | \exp(-i\epsilon \hat{P} \hat{\sigma}_n) | \psi \rangle = F(x, \epsilon, \sigma) \exp\left(\frac{\epsilon x}{2\sigma^2} \hat{\sigma}_n\right), \quad (18)$$

$$\langle p | \exp(-i\epsilon \hat{P} \hat{\sigma}_n) | \psi \rangle = \tilde{\psi}(p) \exp(-i\epsilon p \hat{\sigma}_n). \quad (19)$$

Equation (18) shows the effect of projecting the pointer on x space. The resulting operator on \mathcal{H}_S is, up to a factor, an element of the group $SL(2, C)$. Physically, the latter represents

the action of a filter on a two-level system. By projecting the pointer on p space, Eq. (19) shows that the resulting operator on \mathcal{H}_S is, up to a factor, an element of $SU(2)$. Physically, the latter represents the action of a rotation on a two-level system.

The above remarks connect with results obtained by Brunner *et al.* [26], who showed how weak measurements are incorporated in the daily workings of fiber-optic telecom networks. Brunner *et al.* identified polarization-mode dispersion (PMD) and polarization-dependent losses (PDLs) as two effects that can be related to weak measurements. By tuning PMD, one can go from weak to strong measurements, and by tuning PDLs, one can postselect either pure or mixed polarization states. Whereas PMD is represented by an element of $SU(2)$, PDLs are represented, up to a global attenuation factor, by an element of $SL(2, C)$. Physically, PMD is caused by the birefringence of optical fibers, and PDLs are caused by optical devices having a filtering property, with a polarizer being an extreme case, the one associated with pure states [26]. While there is a connection between Brunner *et al.*’s results and ours, it is important to note that the analysis in [26] was fully conducted in the time domain. The conjugate, the frequency domain, was not invoked. Moreover, PMD and PDLs play two different roles. PMD allows us to move from weak to strong measurements, and PDLs allow us to postselect pure or mixed states. In our case, we have focused on pure states, and the whole process is captured by a single effect, which occurs in one of the two conjugate spaces, the x space or the p space.

In order to further clarify the scope of our description, let us rewrite Eqs. (10) and (12) in terms of the eigenprojectors $|\mathbf{n}_\pm\rangle\langle\mathbf{n}_\pm|$ of $\hat{\sigma}_n$, where $\hat{\sigma}_n|\mathbf{n}_\pm\rangle = \pm|\mathbf{n}_\pm\rangle$. By expressing \hat{I} and $\hat{\sigma}_n$ in terms of the eigenprojectors (see the Appendix), we get

$$\langle x | \exp(-i\epsilon \hat{P} \hat{\sigma}_n) | \psi \rangle = \frac{1}{\sqrt{\sigma}(2\pi)^{1/4}} \left\{ \exp\left[-\frac{(x-\epsilon)^2}{4\sigma^2}\right] |\mathbf{n}_+\rangle\langle\mathbf{n}_+| + \exp\left[-\frac{(x+\epsilon)^2}{4\sigma^2}\right] |\mathbf{n}_-\rangle\langle\mathbf{n}_-| \right\}, \quad (20)$$

$$\langle p | \exp(-i\epsilon \hat{P} \hat{\sigma}_n) | \psi \rangle = \tilde{\psi}(p) \{ \exp(-i\epsilon p) |\mathbf{n}_+\rangle\langle\mathbf{n}_+| + \exp(i\epsilon p) |\mathbf{n}_-\rangle\langle\mathbf{n}_-| \}. \quad (21)$$

Equation (20) allows us to clearly see the two limits, strong and weak, in a von Neumann measurement. With regard to the pointer, we have two Gaussians, centered at $x = \pm\epsilon$, as shown in Fig. 1. Whenever $\epsilon \gg \sigma$, the readout of the pointer is unambiguously correlated with an eigenvalue of $\hat{\sigma}_n$. That is, a readout of the pointer that gives, say, $x = +\epsilon$ is accompanied by a ‘collapse’ of the system to state $|\mathbf{n}_+\rangle$. In the other limit, $\epsilon \ll \sigma$, the two Gaussians overlap (see the left panel of Fig. 1), and a readout of the pointer cannot be unambiguously correlated with an eigenvalue of $\hat{\sigma}_n$. This weak regime has been associated with the weak value σ_n^w . However, as we have seen, σ_n^w can be associated with both weak and strong measurements.

Equation (20) yields, similar to Eq. (10),

$$\frac{\langle f | \langle x | \exp(-i\epsilon \hat{P} \hat{\sigma}_n) | \psi \rangle | i \rangle}{\langle f | i \rangle} = \frac{1}{\sqrt{\sigma}(2\pi)^{1/4}} \left\{ \exp\left[-\frac{(x-\epsilon)^2}{4\sigma^2}\right] \Pi_+^w + \exp\left[-\frac{(x+\epsilon)^2}{4\sigma^2}\right] \Pi_-^w \right\}, \quad (22)$$

where Π_\pm^w are the weak values of the projectors $|\mathbf{n}_\pm\rangle\langle\mathbf{n}_\pm|$. Here again, we use the established nomenclature, even though both weak and strong measurements are equally well described by one and the same expression, Eq. (22).

As for Eq. (21), we can use the explicit expression

$$\tilde{\psi}(p) = \left(\frac{2\sigma^2}{\pi}\right)^{1/4} \exp(-\sigma^2 p^2) \quad (23)$$

to get

$$\frac{\langle f | \langle p | \exp(-i\epsilon \hat{P} \hat{\sigma}_n) | \psi \rangle | i \rangle}{\langle f | i \rangle} = \exp\left(-\frac{\epsilon^2}{4\sigma^2}\right) \left\{ \exp\left[-\left(\sigma p + i\frac{\epsilon}{2\sigma}\right)^2\right] \Pi_+^w + \exp\left[-\left(\sigma p - i\frac{\epsilon}{2\sigma}\right)^2\right] \Pi_-^w \right\}, \quad (24)$$

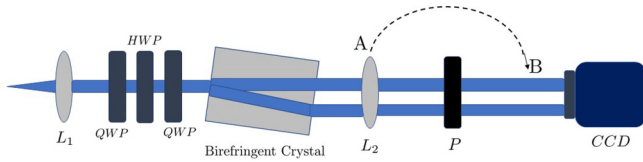


FIG. 2. A source emits a Gaussian beam that is collimated by lens L_1 . Two quarter-wave plates (QWPs) and one half-wave plate (HWP) generate any desired polarization state. The birefringent crystal couples the polarization and optical path, the latter playing the role of the meter in von Neumann's model. A polarizer (P) fixes the postselected polarization state $|f\rangle$. Depending on the position of lens L_2 , the postselected meter state can be position $|x\rangle$ or momentum $|p\rangle$. Setting L_2 on position A, one has a p -imaging lens, while setting L_2 on B, one has an x -imaging lens. In both cases, images form on the CCD, where a single-shot readout is performed.

where we have completed squares to put the result in a form that resembles that of Eq. (22). Despite this formal resemblance, we cannot properly say that we have two Gaussian distributions centered at $p = \pm i\epsilon/2\sigma^2$ because p must be real. We should, however, note that in the literature on weak values, for the sake of brevity authors might say that, e.g., $\exp[-\sigma^2(p - A_w)^2]$ is a Gaussian centered on A_w [4,27] and that $\phi(q - gA_w)$ represents a translation of the wave function by gA_w [28], even though A_w can have complex values.

Instead of writing Eq. (24) in the form of (22), we should rather stress the difference between the two results, (20) and (21), from which they derive. This difference reflects the assumption that our pointer's readouts are positions, i.e., eigenvalues of \hat{X} . In von Neumann's model, the interaction Hamiltonian couples, in this case, the system operator \hat{A} with the meter operator that is conjugate to \hat{X} , i.e., \hat{P} , because it is the latter that causes displacements in the eigenvalues of \hat{X} . Had we chosen to measure the impulse p with our pointer, then we would have taken the Hamiltonian $\hat{H} = g\hat{X}\hat{A}$ to describe the system-meter interaction instead of $\hat{H} = g\hat{P}\hat{A}$. In that case, Eqs. (20) and (21) would interchange their roles.

IV. STOKES POLARIMETRY BASED ON WEAK VALUES

As we have seen, weak values are not restricted to appear in connection with weak measurements. They can also take part in strong measurements. It would be worthwhile, then, to review those cases in which weak values were used under the assumption that the required measurements must be weak. While such a review goes beyond the scope of this work, we want to discuss here a simple method for performing polarimetry, a method that derives from the weak-value approach without fully relying on it, as was the case in Ref. [10].

Let us refer to an optical setup that contains all the essential elements entering weak-value measurements. Following Dressel *et al.* [2], we consider the experiment shown in Fig. 2. The system observable corresponds, in this case, to the polarization degree of freedom, irrespective of the classical or quantum nature of the employed light, e.g., a laser beam or single photons. The system observable couples to a meter operator, which is realized by a birefringent crystal that displaces the light beam in a direction that correlates with the horizontal and vertical components of the polarization state. This is the

optical analog of a Stern-Gerlach experiment with spin-1/2 particles. By tilting the birefringent crystal with respect to the direction of the incident beam, one can vary the length of the path traveled by each polarization component inside the crystal [2]. In this way, one can tune ϵ and span a range that includes both weak and strong measurements.

The system operator \hat{A} is, in this case, represented by the Pauli matrix $\hat{\sigma}_z = |H\rangle\langle H| - |V\rangle\langle V|$, where H refers to horizontal polarization states and V refers to vertical polarization states. The initial state is $|\psi\rangle|i\rangle$, where $|\psi\rangle$ represents the transverse beam profile, and $|i\rangle$ is the polarization state. The postselected meter state can be either $|x\rangle$ or $|p\rangle$, depending on where we put the imaging lens before the detection device. This is a CCD camera, the pixels of which register either the laser intensity or the photon-detection probability. The location of the imaging lens determines whether each pixel corresponds to the transverse position x or to the momentum p . The latter requires the lens to be positioned to work as a Fourier lens.

Let us take the initial polarization state as $|i\rangle = \cos(\alpha/2)|H\rangle + e^{i\beta} \sin(\alpha/2)|V\rangle$ and the final polarization state as $|f\rangle = (|H\rangle - |V\rangle)/\sqrt{2}$. Thus, $|i\rangle$ is the previously mentioned general polarization state [see (7)], whose Stokes vector is $(\cos \beta \sin \alpha, \sin \beta \sin \alpha, \cos \alpha)$. The initial meter state $|\psi\rangle$ represents the Gaussian beam profile that was given in (7). We want to obtain the Stokes vector from our measurements. Such a task is routinely performed with Stokes polarimetry, in which one measures six intensities (or probabilities). These correspond to horizontal, vertical, diagonal, antidiagonal, circular-right, and circular-left polarization states. One must change the settings of some optical devices before recording each intensity. Using the setup in Fig. 2, one must change only once the placement of the imaging lens. The polarizer orientation remains fixed to select only the antidiagonal state $|f\rangle$. The three retarders, i.e., two quarter-wave plates and one half-wave plate set before the birefringent crystal, are there to generate any desired polarization state. Hence, the setup shown serves for the generation and characterization of polarization states. If only the latter is of interest, the setup simplifies to consist of only one imaging lens as an adjustable element. The other elements, the collimating lens, birefringent crystal, polarizer, and CCD camera, remain fixed.

Let us refer first to the intensity or detection probability at pixel x . This is given, up to normalization, by $P_\epsilon(x) = |\langle f|\langle x|\exp(-i\epsilon\hat{P}\hat{\sigma}_z)|\psi\rangle|i\rangle|^2$, which can be readily calculated from (10). As explained in [2], the experimenter can assign a value x or a multiple thereof (see below) to each pixel and thus obtain a centroid that, in our case, is given by

$$C_x = \int xP_\epsilon(x)dx = \frac{\epsilon}{2} \cos \alpha. \quad (25)$$

By setting the lens to work as a Fourier lens, one obtains the centroid in p space. It corresponds to $P_\epsilon(p) = |\langle f|\langle p|\exp(-i\epsilon\hat{P}\hat{\sigma}_z)|\psi\rangle|i\rangle|^2$ and is given by the following expression, which follows from (12):

$$C_p = \int pP_\epsilon(p)dp = \frac{\epsilon}{4\sigma^2} \exp\left(-\frac{\epsilon^2}{2\sigma^2}\right) \sin \beta \sin \alpha. \quad (26)$$

Similarly, one obtains

$$A_p = \int P_\epsilon(p) dp = \frac{1}{2} \left[1 - \exp\left(-\frac{\epsilon^2}{2\sigma^2}\right) \cos \beta \sin \alpha \right]. \quad (27)$$

One can get the Stokes parameters directly by assigning to each pixel values of x or p which are conveniently modified in view of the above equations. For example, regarding (25), instead of x , one assigns the value $2x/\epsilon$ to each pixel and then averages with $P_\epsilon(x)$ [2], thereby obtaining $\cos \alpha$ directly. One proceeds similarly with (26). Alternatively, one can obtain the Stokes parameters as follows:

$$\exp\left(\frac{\epsilon^2}{2\sigma^2}\right)(1 - 2A_p) = \cos \beta \sin \alpha, \quad (28)$$

$$\frac{4\sigma^2}{\epsilon} \exp\left(\frac{\epsilon^2}{2\sigma^2}\right) C_p = \sin \beta \sin \alpha, \quad (29)$$

$$\frac{2}{\epsilon} C_x = \cos \alpha. \quad (30)$$

From the beam profile one gets σ , while the tilting of the birefringent crystal fixes ϵ . These two device parameters should be determined beforehand, following some appropriately designed calibration protocol. We stress that ϵ does not need to be small, a fact that illustrates the usefulness of addressing a model in terms of what it actually contains. Neither weak measurements nor even quantum measurements are necessarily involved when applying von Neumann's model. We see that this model applies beyond its originally intended domain.

V. CONCLUSIONS

The closed-form expressions reported in this work should help us understand the meaning of weak values, a concept that is still under debate. We showed that the standard approach to weak values might be unnecessarily restricted. This approach is based on Taylor expansions of the unitary operator that describes the system-meter interaction in von Neumann's model of quantum measurements. Said Taylor expansions naturally tie together the coupling constant of the interaction Hamiltonian and a system's observable. In the Taylor expansion, increasing orders of weak values are tied to increasing powers of the coupling constant. The closed-form expressions involve only the first-order weak value, which appears as a factor of expressions that contain the coupling parameter. One can then tune large values of the coupling parameter, i.e., perform strong measurements, while still addressing the chosen weak value. In other words, in order to address a weak value, one is not restricted to remain within some weak-measurement regime. The results of this work, which are based on closed-form expressions, complement those of other studies that addressed weak values in connection with strong measurements [15–22].

We stress that most of our findings hold for both quantum and classical systems. Even though the first experimental realization of weak values was conducted with classical light, the prevailing view is that weak values are a purely quantum feature. A similar view probably still prevails about entanglement, despite much theoretical and experimental evidence to the contrary [29–40]. This evidence led Eberly and coworkers

to identify in the very definition of entanglement “a vector-space property, present in any theory with a vector-space framework” [41]. We subscribe to this view and argue that the same should hold for weak values.

ACKNOWLEDGMENTS

This work was partially supported by the U.S. Office of Naval Research Global (ONR, Award No. N62909-19-1-2148, Grant No. GRANT12853637).

APPENDIX: CLOSED-FORM EXPRESSIONS OF MATRIX EXPONENTIALS

Let \hat{A} be a Hermitian operator with eigenvalues a_n and eigenvectors $|a_n\rangle$, and let $f(z)$ be an analytic function. It then holds that $f(\hat{A})$, which is defined in terms of the series expansion of $f(z)$, can also be written as $f(\hat{A}) = \sum_n f(a_n) |a_n\rangle \langle a_n|$. Consider the Pauli operator $\hat{\sigma}_n = \mathbf{n} \cdot \boldsymbol{\sigma}$, whose eigenvectors we denote by $|\mathbf{n}_\pm\rangle$. We have then that $\theta \hat{\sigma}_n |\mathbf{n}_\pm\rangle = \pm \theta |\mathbf{n}_\pm\rangle$. Let θ be a quantity that commutes with $\hat{\sigma}_n$. Then, setting $\hat{A} = \theta \hat{\sigma}_n$ in the formula above, we get

$$f(\theta \hat{\sigma}_n) = f(\theta) |\mathbf{n}_+\rangle \langle \mathbf{n}_+| + f(-\theta) |\mathbf{n}_-\rangle \langle \mathbf{n}_-|. \quad (A1)$$

Moreover,

$$\hat{I} = |\mathbf{n}_+\rangle \langle \mathbf{n}_+| + |\mathbf{n}_-\rangle \langle \mathbf{n}_-|, \quad (A2)$$

$$\hat{\sigma}_n = |\mathbf{n}_+\rangle \langle \mathbf{n}_+| - |\mathbf{n}_-\rangle \langle \mathbf{n}_-|. \quad (A3)$$

Hence, we can write (A1) in the form

$$f(\theta \hat{\sigma}_n) = \frac{1}{2} [f(\theta) + f(-\theta)] \hat{I} + \frac{1}{2} [f(\theta) - f(-\theta)] \hat{\sigma}_n. \quad (A4)$$

We are interested in the evolution operator $U(\epsilon) = \exp(-i\epsilon \hat{P} \hat{\sigma}_n) \equiv \exp(-ig\tau \hat{P} \hat{\sigma}_n)$ of the interaction Hamiltonian $\hat{H} = g\hat{P} \otimes \hat{\sigma}_n$. Here, \hat{P} and $\hat{\sigma}_n$ commute with one another because they act on different subspaces (strictly, $\hat{P} \otimes \hat{I}$ commutes with $\hat{I} \otimes \hat{\sigma}_n$). Thus, as long as the system S is concerned, a meter operator $\theta \equiv \epsilon \hat{P}$ behaves as a c number rather than as a q number. Hence, (A4) holds for $f(\theta \hat{\sigma}_n) = \exp(-i\theta \hat{\sigma}_n)$, so that

$$\exp(-i\theta \hat{\sigma}_n) = \frac{1}{2} \{ (e^{-i\theta} + e^{i\theta}) \hat{I} + (e^{-i\theta} - e^{i\theta}) \hat{\sigma}_n \}. \quad (A5)$$

\hat{P} acts as a derivative in the x representation: $\langle x | \hat{P} | \psi \rangle = -i\partial \psi / \partial x$. Hence, $\langle x | \pm i\theta | \psi \rangle = \pm \epsilon \partial \psi / \partial x$, so that Taylor expansion of $e^{\pm i\theta}$ leads to

$$\langle x | (e^{-i\theta} \pm e^{i\theta}) | \psi \rangle = \sum_k \left[\frac{(-\epsilon)^k}{k!} \frac{\partial^k \psi}{\partial x^k} \pm \frac{\epsilon^k}{k!} \frac{\partial^k \psi}{\partial x^k} \right]. \quad (A6)$$

In our case, $\psi(x) = \langle x | \psi \rangle = (2\pi\sigma^2)^{-1/4} \exp(-x^2/4\sigma^2)$. It is convenient to define

$$G(x, \sigma) = |\psi(x)|^2 = \frac{1}{\sigma\sqrt{2\pi}} \exp(-x^2/2\sigma^2). \quad (A7)$$

The k th derivative of $G(x, \sigma)$ is proportional to the k th Hermite polynomial $H_k(x)$:

$$\frac{\partial^k G(x, \sigma)}{\partial x^k} = \left(\frac{-1}{\sigma\sqrt{2}} \right)^k H_k \left(\frac{x}{\sigma\sqrt{2}} \right) G(x, \sigma). \quad (A8)$$

From this, it follows that

$$\sum_{k=0}^{\infty} \frac{(\mp\epsilon)^k}{k!} \frac{\partial^k \psi}{\partial x^k} = \sqrt{2\sigma} (2\pi)^{1/4} \sum_{k=0}^{\infty} \frac{(\pm\epsilon/2\sigma)^k}{k!} H_k\left(\frac{x}{2\sigma}\right) G(x, \sigma\sqrt{2}). \quad (\text{A9})$$

We recall that Hermite polynomials can be defined through their generating function:

$$\exp(-t^2 + 2tx) = \sum_{k=0}^{\infty} \frac{t^k}{k!} H_k(x). \quad (\text{A10})$$

On comparing (A10) and (A9), we see that

$$\sum_{k=0}^{\infty} \frac{(\mp\epsilon)^k}{k!} \frac{\partial^k \psi}{\partial x^k} = \sqrt{2\sigma} (2\pi)^{1/4} \exp\left[-\left(\frac{\epsilon}{2\sigma}\right)^2 \pm \frac{\epsilon x}{2\sigma^2}\right] G(x, \sigma\sqrt{2}). \quad (\text{A11})$$

Equation (A11) can be used in (A6) to obtain

$$\langle x | (e^{-i\theta} + e^{i\theta}) | \psi \rangle = 2\sqrt{2\sigma} (2\pi)^{1/4} \exp\left[-\left(\frac{\epsilon}{2\sigma^2}\right)^2\right] G(x, \sigma\sqrt{2}) \cosh\left(\frac{\epsilon x}{2\sigma^2}\right), \quad (\text{A12})$$

$$\langle x | (e^{-i\theta} - e^{i\theta}) | \psi \rangle = 2\sqrt{2\sigma} (2\pi)^{1/4} \exp\left[-\left(\frac{\epsilon}{2\sigma^2}\right)^2\right] G(x, \sigma\sqrt{2}) \sinh\left(\frac{\epsilon x}{2\sigma^2}\right). \quad (\text{A13})$$

The above results, together with (A5) and (A6), lead to

$$\langle x | \exp(-i\theta \hat{\sigma}_n) | \psi \rangle = \sqrt{2\sigma} (2\pi)^{1/4} \exp\left(-\frac{\epsilon^2}{4\sigma^2}\right) G(x, \sigma\sqrt{2}) \left\{ \cosh\left(\frac{\epsilon x}{2\sigma^2}\right) \hat{f} + \sinh\left(\frac{\epsilon x}{2\sigma^2}\right) \hat{\sigma}_n \right\}. \quad (\text{A14})$$

As for the p representation, we have

$$\langle p | (e^{-i\theta} + e^{i\theta}) | \psi \rangle = \langle p | (e^{-i\epsilon p} + e^{i\epsilon p}) | \psi \rangle = 2\langle p | \cos(\epsilon p) | \psi \rangle, \quad (\text{A15})$$

$$\langle p | (e^{-i\theta} - e^{i\theta}) | \psi \rangle = \langle p | (e^{-i\epsilon p} - e^{i\epsilon p}) | \psi \rangle = -2i\langle p | \sin(\epsilon p) | \psi \rangle. \quad (\text{A16})$$

Hence,

$$\langle p | \exp(-i\theta \hat{\sigma}_n) | \psi \rangle = \tilde{\psi}(p) \{ \cos(\epsilon p) \hat{f} - i \sin(\epsilon p) \hat{\sigma}_n \}. \quad (\text{A17})$$

-
- [1] Y. Aharonov, D. Z. Albert, and L. Vaidman, How the Result of a Measurement of a Component of the Spin of a Spin-1/2 Particle Can Turn Out to be 100, *Phys. Rev. Lett.* **60**, 1351 (1988).
- [2] J. Dressel, M. Malik, F. M. Miatto, A. N. Jordan, and R. W. Boyd, Colloquium: Understanding quantum weak values: Basics and applications, *Rev. Mod. Phys.* **86**, 307 (2014).
- [3] A. Hariri, D. Curic, L. Giner, and J. S. Lundeen, Experimental simultaneous readout of the real and imaginary parts of the weak value, *Phys. Rev. A* **100**, 032119 (2019).
- [4] I. M. Duck, P. M. Stevenson, and E. C. G. Sudarshan, The sense in which a “weak measurement” of a spin-1/2 particle’s spin component yields a value 100, *Phys. Rev. D* **40**, 2112 (1989).
- [5] O. Hosten and P. Kwiat, Observation of the spin-Hall effect of light via weak measurements, *Science* **319**, 787 (2008).
- [6] J. S. Lundeen, B. Sutherland, A. Patel, C. Stewart, and C. Bamber, Direct measurement of the quantum wavefunction, *Nature (London)* **474**, 188 (2011).
- [7] J. P. Groen, D. Riste, L. Tornberg, J. Cramer, P. C. de Groot, T. Picot, G. Johansson, and L. DiCarlo, Partial-Measurement Backaction and Nonclassical Weak Values in a Superconducting Circuit, *Phys. Rev. Lett.* **111**, 090506 (2013).
- [8] S. Kocsis, B. Braverman, S. Ravets, M. J. Stevens, R. P. Mirin, L. K. Shalm, and A. M. Steinberg, Observing the Average Trajectories of Single Photons in a Two-Slit Interferometer, *Science* **332**, 1170 (2011).
- [9] D. H. Mahler, L. Rozema, K. Fisher, L. Vermeyden, K. J. Resch, H. W. Wiseman, and A. Steinberg, Experimental nonlocal and surreal Bohmian trajectories, *Sci. Adv.* **2**, e1501466 (2016).
- [10] J. Z. Salvail, M. Agnew, A. S. Johnson, E. Bolduc, J. Leach, and R. W. Boyd, Full characterization of polarization states of light via direct measurement *Nat. Photonics* **7**, 316 (2013).
- [11] H. Kobayashi, K. Nonaka, and Y. Shikano, Stereographical visualization of a polarization state using weak measurements with an optical-vortex beam, *Phys. Rev. A* **89**, 053816 (2014).
- [12] W. M. Itano, D. J. Heinzen, J. J. Bollinger, and D. J. Wineland, Quantum Zeno effect, *Phys. Rev. A* **41**, 2295 (1990).
- [13] N. W. M. Ritchie, J. G. Story, and R. G. Hulet, Realization of a Measurement of a “Weak Value,” *Phys. Rev. Lett.* **66**, 1107 (1991).
- [14] G. J. Pryde, J. L. O’Brien, A. G. White, T. C. Ralph, and H. M. Wiseman, Measurement of Quantum Weak Values of Photon Polarization, *Phys. Rev. Lett.* **94**, 220405 (2005).
- [15] A. Di Lorenzo, Full counting statistics of weak-value measurement, *Phys. Rev. A* **85**, 032106 (2012).

- [16] A. G. Kofman, S. Ashhab, and F. Nori, Nonperturbative theory of weak pre- and postselected measurements, *Phys. Rep.* **520**, 43 (2012).
- [17] G. Vallone and D. Dequal, Strong Measurements Give a Better Direct Measurement of the Quantum Wave Function, *Phys. Rev. Lett.* **116**, 040502 (2016).
- [18] T. Denkmayr, H. Geppert, H. Lemmel, M. Waegell, J. Dressel, Y. Hasegawa, and S. Sponar, Experimental Demonstration of Direct Path State Characterization by Strongly Measuring Weak Values in a Matter-Wave Interferometer, *Phys. Rev. Lett.* **118**, 010402 (2017).
- [19] E. Cohen and E. Pollak, Determination of weak values of quantum operators using only strong measurements, *Phys. Rev. A* **98**, 042112 (2018).
- [20] L. Calderaro, G. Foletto, D. Dequal, P. Villoresi, and G. Vallone, Direct Reconstruction of the Quantum Density Matrix by Strong Measurements, *Phys. Rev. Lett.* **121**, 230501 (2018).
- [21] J. Dziewior, L. Knips, D. Farfurnik, K. Senkalla, N. Benschalom, J. Efroni, J. Meinecke, S. Bar-Ad, H. Weinfurter, and L. Vaidman, Universality of local weak interactions and its application for interferometric alignment, *Proc. Natl. Acad. Sci. USA* **116**, 2881 (2019).
- [22] K. Ogawa, N. Abe, H. Kobayashi, and A. Tomita, Complex counterpart of variance in quantum pre- and postselected systems, *Phys. Rev. Res.* **3**, 033077 (2021).
- [23] L. Vaidman, A. Ben-Israel, J. Dziewior, L. Knips, M. Weiß, J. Meinecke, C. Schwemmer, R. Ber, and H. Weinfurter, Weak value beyond conditional expectation value of the pointer readings, *Phys. Rev. A* **96**, 032114 (2017).
- [24] K. Ogawa, H. Kobayashi, and A. Tomita, Operational formulation of weak values without probe systems, *Phys. Rev. A* **101**, 042117 (2020).
- [25] A. Di Lorenzo, Strong correspondence principle for joint measurement of conjugate observables, *Phys. Rev. A* **83**, 042104 (2011).
- [26] N. Brunner, A. Acín, D. Collins, N. Gisin, and V. Scarani, Optical Telecom Networks as Weak Quantum Measurements with Postselection, *Phys. Rev. Lett.* **91**, 180402 (2003).
- [27] J. S. Lundeen and K. J. Resch, Practical measurement of joint weak values and their connection to the annihilation operator, *Phys. Lett. A* **334**, 337 (2005).
- [28] R. Jozsa, Complex weak values in quantum measurements, *Phys. Rev. A* **76**, 044103 (2007).
- [29] R. J. C. Spreeuw, A classical analogy of entanglement, *Found. Phys.* **28**, 361 (1998).
- [30] A. Luis, Coherence, polarization, and entanglement for classical fields, *Opt. Commun.* **282**, 3665 (2009).
- [31] B. N. Simon, S. Simon, F. Gori, M. Santarsiero, R. Borghi, N. Mukunda, and R. Simon, Nonquantum Entanglement Resolves a Basic Issue in Polarization Optics, *Phys. Rev. Lett.* **104**, 023901 (2010).
- [32] C. V. S. Borges, M. Hor-Meyll, J. A. O. Huguénin, and A. Z. Khoury, Bell-like inequality for the spin-orbit separability of a laser beam, *Phys. Rev. A* **82**, 033833 (2010).
- [33] X.-F. Qian and J. H. Eberly, Entanglement and classical polarization states, *Opt. Lett.* **36**, 4110 (2011).
- [34] K. H. Kagalwala, G. DiGiuseppe, A. F. Abouraddy, and B. E. A. Saleh, Bell's measure in classical optical coherence, *Nat. Photonics* **7**, 72 (2013).
- [35] A. Aiello, F. Töppel, C. Marquardt, E. Giacobino, and G. Leuchs, Quantum-like nonseparable structures in optical beams, *New J. Phys.* **17**, 043024 (2015).
- [36] X.-F. Qian, T. Malhotra, A. N. Vamivakas, and J. H. Eberly, Coherence Constraints and the Last Hidden Optical Coherence, *Phys. Rev. Lett.* **117**, 153901 (2016).
- [37] J. H. Eberly, Correlation, coherence and context, *Laser Phys.* **26**, 084004 (2016).
- [38] N. Dgano, B. Perez-Garcia, F. S. Roux, M. McLaren, C. Rosales-Guzman, Y. Zhang, O. Mouane, R. I. Hernandez-Aranda, T. Konrad, and A. Forbes, Characterizing quantum channels with nonseparable states of classical light, *Nat. Phys.* **13**, 397 (2017).
- [39] A. Al-Qasimi, Coherence, entanglement, and complementarity in mixed classical light, *J. Opt. Soc. Am. A* **37**, 1526 (2020).
- [40] T. Qureshi, Predictability, distinguishability and entanglement, *Opt. Lett.* **46**, 492 (2021).
- [41] J. H. Eberly, X.-F. Qian, A. Al Qasimi, H. Ali, M. A. Alonso, R. Gutiérrez-Cuevas, B. J. Little, J. C. Howell, T. Malhotra, and A. N. Vamivakas, Quantum and classical optics - emerging links, *Phys. Scr.* **91**, 063003 (2016).